



RESEARCH PAPER

SLAH1, a homologue of the slow type anion channel SLAC1, modulates shoot Cl^- accumulation and salt tolerance in *Arabidopsis thaliana*

Jiaen Qiu^{1,2,3}, Sam W Henderson^{1,3}, Mark Tester⁴, Stuart J Roy^{1,2} and Mathew Gilliham^{1,3,*}

¹ School of Agriculture, Food, and Wine, University of Adelaide, PMB1, Glen Osmond, SA 5064, Australia

² Australian Centre for Plant Functional Genomics, PMB1, Glen Osmond, SA 5064, Australia

³ ARC Centre of Excellence in Plant Energy Biology, PMB1, Glen Osmond, SA 5064, Australia

⁴ Centre for Desert Agriculture, King Abdullah University of Science and Technology, Thuwal 23955–6900, Kingdom of Saudi Arabia

* Correspondence: matthew.gilliham@adelaide.edu.au

Received 19 April 2016; Accepted 25 May 2016

Editor: Karl-Josef Dietz, Bielefeld University

Abstract

Salinity tolerance is correlated with shoot chloride (Cl^-) exclusion in multiple crops, but the molecular mechanisms of long-distance Cl^- transport are poorly defined. Here, we characterize the *in planta* role of AtSLAH1 (a homologue of the slow type anion channel-associated 1 (SLAC1)). This protein, localized to the plasma membrane of root stelar cells, has its expression reduced by salt or ABA, which are key predictions for a protein involved with loading Cl^- into the root xylem. Artificial microRNA knockdown mutants of AtSLAH1 had significantly reduced shoot Cl^- accumulation when grown under low Cl^- , whereas shoot Cl^- increased and the shoot nitrate/chloride ratio decreased following AtSLAH1 constitutive or stelar-specific overexpression when grown in high Cl^- . In both sets of overexpression lines a significant reduction in shoot biomass over the null segregants was observed under high Cl^- supply, but not low Cl^- supply. Further *in planta* data showed AtSLAH3 overexpression increased the shoot nitrate/chloride ratio, consistent with AtSLAH3 favouring nitrate transport. Heterologous expression of AtSLAH1 in *Xenopus laevis* oocytes led to no detectable transport, suggesting the need for post-translational modifications for AtSLAH1 to be active. Our *in planta* data are consistent with AtSLAH1 having a role in controlling root-to-shoot Cl^- transport.

Key words: ABA, Arabidopsis, AtSLAH1, AtSLAH3, chloride, Cl^- xylem loading, long-distance transport, nutrition, salinity, slow-type anion channel-associated homologue 1, slow-type anion channel-associated homologue 3.

Introduction

Chloride (Cl^-) is classified as a micronutrient, but it is often present in plant tissues at concentrations typical of a macronutrient (i.e. 2–20 rather than 0.1–200 $\mu\text{g g}^{-1}$ DW) (Marschner, 1995; Xu *et al.*, 2000; Broadley *et al.*, 2012; Franco-Navarro *et al.*, 2015). Cl^- has vital roles in regulating numerous physiological processes including turgor, enzyme activity, photosynthesis and membrane potential (Rognes,

1980; White and Broadley, 2001; Teakle and Tyerman, 2010). Although the pathways for Cl^- entry and movement within the plant have been characterized biochemically, their molecular determinants are poorly defined (Teakle and Tyerman, 2010; Henderson *et al.*, 2014).

High concentrations of sodium chloride (NaCl) in soils reduces crop yield (Rengasamy, 2010; Roy *et al.*, 2014), which

can impose significant economic costs to farmers (Munns and Gilliham, 2015). Na^+ transport and its impact on plant growth have been relatively well documented at both a physiological and a molecular level in a variety of plant species (Blumwald *et al.*, 2000; Zhu, 2003; Horie and Schroeder, 2004; Davenport *et al.*, 2005; Garthwaite *et al.*, 2005; Chinnusamy *et al.*, 2006; Apse and Blumwald, 2007; Horie *et al.*, 2008; Müller *et al.*, 2014; Roy *et al.*, 2014; Maathuis *et al.*, 2014; Flowers *et al.*, 2015). However, in other economically important crop plants like soybean, grapevine, citrus and lotus, leaf Cl^- accumulation (not Na^+) is correlated with decreased plant growth and photosynthesis when plants are under salt stress (Storey and Walker, 1999; Walker *et al.*, 2002; Tregeagle *et al.*, 2006; Teakle *et al.*, 2007; Teakle and Tyerman, 2010; Gong *et al.*, 2011). So, although Cl^- is a micronutrient it can also accumulate to concentrations that inhibit plant growth when plants encounter salinity. The cause of both Na^+ - and Cl^- -induced reductions in photosynthesis and growth, and the cause of salt-induced cell death are yet to be definitively determined and are a priority area for research (Munns and Gilliham, 2015). Some studies have investigated the relative impact of Na^+ and Cl^- on barley and wheat (e.g. Tavakkoli *et al.*, 2011; Genc *et al.*, 2015). Growth and photosynthesis of several cultivars of barley appeared to be more sensitive to the addition of Cl^- than of Na^+ (Tavakkoli *et al.*, 2011). These findings highlight the importance of investigating the regulation of both Na^+ and Cl^- transport for improving plant salt tolerance, even in species that are classically considered to be more Na^+ -sensitive than Cl^- -sensitive under saline conditions.

Identification of genes that underpin root-to-shoot Cl^- transport, and the related signalling pathways, should provide information that could be used to reduce Cl^- sensitivity in commercial crops. A key pathway in controlling Cl^- accumulation in the shoot is its loading from xylem parenchyma cells into the transpiration stream (Teakle and Tyerman, 2010). Recently, a nitrate (NO_3^-) transporter 1/peptide transporter family member (*NPF2.4*) was identified as the first protein to be directly involved in loading Cl^- into the root xylem (Li *et al.*, 2016). However, Cl^- accumulation in the shoot is predicted to be a multigenic trait in a number of plant groups and species including soybean, maize, grapevine, citrus and legumes (Abel, 1969; Storey and Walker, 1999; Moya *et al.*, 2003; Sibole *et al.*, 2003; Gilliham and Tester, 2005; Gong *et al.*, 2011; Henderson *et al.*, 2014; Fort *et al.*, 2015). Knockouts of *Atnpt2.4* had a 20% reduction in shoot Cl^- (Li *et al.*, 2016), providing further evidence of the multigenic nature of shoot Cl^- accumulation. Therefore, other anion transport proteins are likely to be involved in root-to-shoot Cl^- transport (e.g. Henderson *et al.*, 2014), but these remain to be identified and functionally characterized at a molecular level.

Three anion conductances have been identified using electrophysiology in barley root xylem parenchyma protoplasts, namely an inwardly rectifying anion channel (X-IRAC), a quickly activating anion conductance (X-QUAC) and a slowly activating anion conductance (X-SLAC) (Köhler and Raschke, 2000). Similar results were found in maize root stelar cells (Gilliham and Tester, 2005) and Arabidopsis root pericycle cells (Kiegle *et al.*, 2000). X-QUAC is the most

prevalent conductance observed in xylem parenchyma cells and is likely to load the majority of Cl^- (and NO_3^-) ions into the xylem under non-saline conditions (Köhler *et al.*, 2002; Gilliham and Tester, 2005) as the estimated flux through this conductance could easily account for the Cl^- release from the xylem vessels measured using a $^{36}\text{Cl}^-$ tracer (Pitman, 1982; Köhler and Raschke, 2000).

The hormone abscisic acid (ABA) regulates solute transport from root to shoot (Cram and Pitman, 1972). Excised barley roots treated with ABA for 2 h accumulated significantly more Cl^- than untreated roots (Cram and Pitman, 1972). Cl^- efflux to the xylem was also reduced following the ABA treatment, but Cl^- influx into the root was unaffected (Cram and Pitman, 1972). These results indicate that ABA down-regulates xylem loading of Cl^- in roots but not root Cl^- influx. Furthermore, the anion conductances in maize, barley and Arabidopsis stele, as well as the potassium conductance through the stelar K^+ outwardly rectifying channel (SKOR), are also down-regulated by ABA (Cram and Pitman, 1972; Gilliham and Tester, 2005). In Arabidopsis, *AtSKOR* was transcriptionally down-regulated by ABA (Gaymard *et al.*, 1998). Therefore, it may be possible to identify candidate genes for Cl^- loading into the root xylem by characterizing those genes encoding putative anion transporters that are expressed in the stele and are down-regulated (either transcriptionally or post-translationally) by ABA.

Early electrophysiological studies on stomatal guard cells revealed the slowly activated anion conductance (SLAC) (Linder and Raschke, 1992). More recently, the gene encoding the protein responsible for this conductance, *SLAC1*, was identified (Negi *et al.*, 2008; Vahisalu *et al.*, 2008). *SLAC1* is a plasma membrane (PM) localized protein, highly permeable to malate and chloride (Negi *et al.*, 2008; Chen *et al.*, 2010), and *slac1* mutants have increased Cl^- in guard cells (Negi *et al.*, 2008; Vahisalu *et al.*, 2008). Four homologues of *SLAC1*, the slow-type anion channel-associated homologues 1 to 4 (SLAH1 to 4), have been identified that also localize to the PM and are predicted to be involved in anion transport (Negi *et al.*, 2008; Vahisalu *et al.*, 2008). Expression of *SLAH1* or *SLAH3* in *slac1* knockout mutants could complement both the defective closure response of *slac1* stomata to high CO_2 and its ionic profile when constitutively overexpressed (Negi *et al.*, 2008). *SLAH3* is expressed in guard cells and roots, and is preferentially selective for NO_3^- over Cl^- ; it has a role in NO_3^- alleviation of ammonium toxicity (Geiger *et al.*, 2009, 2011; Demir *et al.*, 2013; Zheng *et al.*, 2015). *SLAH2* is also expressed in roots (Maierhofer *et al.*, 2014), and the protein is predominantly permeable to NO_3^- (with a $\text{NO}_3^-/\text{Cl}^-$ permeability ratio of 82) (Maierhofer *et al.*, 2014). Both *SLAH2* and *SLAH3* have been predicted to have roles in loading NO_3^- into the root xylem (Maierhofer *et al.*, 2014; Zheng *et al.*, 2015). *SLAH1* is also expressed in the root; however, the role of *AtSLAH1* is currently unknown. As *SLAH1* is expressed in the root stele and can complement the stomatal phenotype of the *Atslac1* mutant when ectopically expressed (Negi *et al.*, 2008; Vahisalu *et al.*, 2008; Zheng *et al.*, 2015), we examined whether *AtSLAH1* has a role in loading Cl^- into the root xylem.

Materials and methods

Plant materials and growth conditions

All chemicals were obtained from Sigma-Aldrich unless stated. *Arabidopsis thaliana* ecotype (Col-0) seeds were purchased from the European Arabidopsis Stock Centre (Nottingham, UK). Plants were grown within temperature controlled growth rooms. Arabidopsis plants grown in soil were kept in long day conditions (16h day/8h night), while those in hydroponics were kept in short day conditions (10h day/14h night). In both long day and short day conditions, the temperature was maintained at 21–23 °C, the humidity was maintained between 60–75%, and the irradiance during the light period was 150 μmol m⁻² s⁻¹. Plants were grown in hydroponics following protocols described in Conn *et al.* (2013) and in soil following methods described in Møller *et al.* (2009).

Generation of AtSLAH1 artificial microRNA lines

The *AtSLAH1* T-DNA knockout mutant (FLAG_329G06) was ordered through the Versailles Arabidopsis Stock Centre; however, the expression of *AtSLAH1* (At1G62280) was detectable in all homozygous mutant lines (Supplementary Fig. S1 at JXB online). To elucidate the function of *AtSLAH1* in planta, artificial microRNAs (amiRNAs) were designed to knockdown *AtSLAH1* expression. To produce *AtSLAH1* knockdown mutants, specific amiRNAs were designed against the *AtSLAH1* mRNA sequence using Micro RNA Designer (<http://wmd3.weigelworld.org/cgi-bin/webapp.cgi>) following the protocol of Schwab *et al.* (2006). Two 21 bp target sequences (TAAACGCTATTTGGTCCGT and TTATGTCTAGTGTGCGAGACTG) were identified from the *AtSLAH1* coding sequence and two independent amiRNA constructs were generated with a set of primers (Supplementary Table S1) to incorporate the 21 bp amiRNA sequence into the MIR319a vector (Schwab *et al.*, 2006). Both full-length *SLAH1*-amiRNA products were cloned using high-fidelity Phusion® polymerase (New England Biolabs, USA) into a Gateway® enabled pCR8 entry vector (Invitrogen, CA, USA) and transferred into the pMDC32 expression vector (Curtis and Grossniklaus, 2003) through an LR reaction (Invitrogen). The constructs were transformed into Arabidopsis using Agrobacterium-mediated floral dip transformation (Clough and Bent, 1998). Hygromycin B (20 μg ml⁻¹) was used to select the transformants following the protocol described in Harrison *et al.* (2006).

Generation of cell type-specific overexpression lines

An Arabidopsis enhancer trap line (E2568; Møller *et al.*, 2009) was used to generate plants with *AtSLAH1* root stelar-cell-specific overexpression. *AtSLAH1* full length cDNA was cloned using high-fidelity Phusion® polymerase (New England Biolabs, USA) from Arabidopsis root cDNA (following RNA extraction and cDNA synthesis following Henderson *et al.* (2015)) into a Gateway-enabled pCR8 entry vector (Life Technologies, CA, USA). *AtSLAH1* was then transferred into a pTOOL5 destination vector (pMDC132+UAS+NOS) (Plett, 2008) containing the GAL4-inducible promoter UAS, which drives target gene expression specifically in root stelar cells in line E2568. The construct was transformed into Arabidopsis line E2586 using Agrobacterium-mediated transformation (Clough and Bent, 1998). The seeds from transformed plants were harvested and germinated in soil. When the seedling had two to four true leaves, 20 mg l⁻¹ BASTA (Bayer, Germany) was sprayed on the seedlings to select for plants with the transgenic insertion.

Generation of constitutive overexpression lines

Full-length *AtSLAH1* and *AtSLAH3* coding sequences were amplified (the primers used are listed in Supplementary Table S1) from Arabidopsis root cDNA, using Phusion® polymerase, cloned into the

Gateway-enabled pCR8 entry vector (Life Technologies) and transferred into the pMDC32 expression vector (Curtis and Grossniklaus, 2003) through an LR reaction (Life Technologies). The construct was transformed into Arabidopsis (Col-0) using Agrobacterium-mediated transformation (Clough and Bent, 1998). Hygromycin B (20 μg ml⁻¹) was used to select lines containing the transgene insertion following the protocol described in Harrison *et al.* (2006).

Salinity and ABA treatment

Both salinity and ABA treatment were performed in hydroponics (Conn *et al.*, 2013). For the 7-day salinity treatment, NaCl was added to basal nutrient solution (BNS) (Conn *et al.*, 2013) to make a final concentration of 50, 75, and 100 mM. Additional CaCl₂ was added to each solution to achieve a constant Ca²⁺ activity of 1.3 mM following the addition of high concentrations of monovalent cations, which act to reduce the activity of other cations and induce calcium deficiency (as detailed in Conn *et al.* (2013)). For ABA treatment, a stock solution of 100 mM (±)-*cis-trans*-abscisic acid was made in absolute ethanol. When applying 20 μM ABA, this resulted in a final ethanol concentration of 0.01% (v/v) when added into the growth solution.

Expression analysis

Gene expression analysis by qRT-PCR was performed following the method described in Burton *et al.* (2008). The primers for examining *AtSLAH1* expression were 5'TCTTCATGTCCCTGGTCTG3' (forward) and 5'ATTGCTGTTTGCTGCTGTC3' (reverse) and for *AtSLAH3* were 5'ATCTCTCGGTGCTGGGAACCTTTG3' (forward) and 5'CTCGTTGGTTCGGTAGCCTTTGG3' (reverse). The selected Arabidopsis housekeeping genes (*AtGAPDH* (At3G26650), *AtActin2* (At3G18780), *AtTubulin* (At1G50010) and *AtCyclophilin* (At2G36130)) and data normalization followed the methods described in Jha *et al.* (2010). For relative gene expression, *AtActin2* was used as a control gene, and the relative expression level of target genes was detected using the same primer pairs as listed above using a QuantStudio 12K Flex Real-Time PCR system (Life Technologies).

Phenotyping transgenic plants

For determining the shoot NO₃⁻ concentration, a method that uses salicylic acid to form a chromophore with NO₃⁻ under alkaline conditions (pH>12) was used (Cataldo *et al.*, 1975). In brief, 3–5 mg of Arabidopsis dried tissue was extracted in 0.5 ml deionized water, with 0.05 ml of the extraction incubated with 0.2 ml of 5% (w/v) salicylic acid–H₂SO₄ for 20 min at room temperature; 0.05 ml of this mixture was transferred into a fresh tube and 0.95 ml of 2 M NaOH was added. A 0.2 ml aliquot was transferred to a well of a transparent 96-well plate and the absorbance at OD_{410nm} determined. A serial dilution of known concentrations of potassium nitrate (KNO₃) was used for the standard, which ranged from 0 to 50 mM.

For determining the shoot Cl⁻ concentration, 20–30 mg of freeze-dried Arabidopsis tissue was extracted in 500 μl 1% nitric acid at 80 °C overnight. A chloride analyser (Model 926S, Sherwood Scientific, Cambridge, UK) was used to examine the Cl⁻ concentration by following the manufacturer's instructions.

Expression and electrophysiological characterization of AtSLAH1 in *X. laevis* oocytes

The *AtSLAH1*, *AtSnRK2.2*, and *AtSnRK2.3* coding sequences (primers are listed in Supplementary Table S1) were cloned using high-fidelity Phusion® polymerase (New England Biolabs, USA) from Arabidopsis root cDNA into a Gateway-enabled pCR8 entry vector (Life Technologies) before being transferred into the pGEM-HE (DEST) vector, and cRNA was synthesized using the mMESSAGE mMACHINE® kit (Ambion, Australia) as previously described (Preuss *et al.*, 2011). Healthy stage IV–VI defolliculated oocytes were obtained through surgery and enzymatic digestion of ovaries from toads kept

in an *Xenopus* colony at the Waite Campus (University of Adelaide). The cRNA (46 nl/23 ng per oocyte) was injected using a micro injector (Drummond Nanoject II injector, USA) with a glass microcapillary pipette following the manufacturer's procedures. The same volume of nuclease-free water was injected into control oocytes. Injected oocytes were incubated at 18 °C for 2 days in an ND96 solution (96 mM NaCl, 2 mM KCl, 1 mM MgCl₂, 5 mM 4-(2-hydroxyethyl)-1-piperazineethanesulfonic acid (HEPES), 1.8 mM CaCl₂, pH 7.4 with 1 M Tris) combined with horse serum (50 ml l⁻¹), tetracycline (50 µg ml⁻¹) and penicillin (50 µg ml⁻¹). After 2 days, *AtSLAH1* cRNA-injected oocytes were voltage clamped from +40 to -120 mV in 20 mV decrements for 3 s perfusing in the following bath solutions (basal: 2 mM calcium gluconate, 5 mM HEPES and 0.1 mM LaCl₃) plus 1 or 20 mM CsNO₃/CsCl at pH 7.5. Two-electrode voltage clamping (TEVC) was performed on oocytes as previously described in Roy *et al.* (2008) using an OC-725C amplifier (Warner Instruments Corp., USA), signals were digitized with a Digidata 1440A (Molecular Devices, USA), and then the data were recorded and analysed using pCLAMP 10.2 (Molecular Devices, USA).

Results

AtSLAH1 expression is down-regulated by both salt and ABA

A qRT-PCR was performed on Arabidopsis root cDNA to determine whether *AtSLAH1* transcript abundance altered following salt or ABA treatment. The expression level of *AtSLAH1* was significantly reduced by 91% after 7 days of 100 mM NaCl treatment, and by 97% after 16 h of 20 µM ABA treatment when compared with the control (Fig. 1A). In contrast, the close homologue *AtSLAH3*, which shares the same cell location in xylem parenchyma and pericycle cells of the root stele and is also PM localized (Negi *et al.*, 2008), was not down-regulated by ABA or salt treatment (Fig. 1B). All these data are consistent with previous observations (Kilian *et al.*, 2007; Brady *et al.*, 2007; Gifford *et al.*, 2008; Supplementary Fig. S2).

AtSLAH1 amiRNA knockdown lines have low Cl⁻ accumulation in the shoot under low Cl⁻ supply

To investigate whether *AtSLAH1* was involved in root-to-shoot anion transport, different Arabidopsis lines with an increase or decrease in *AtSLAH1* expression were generated.

Atslah1 knockout lines (FLAG_329G06) were ordered from the Versailles Arabidopsis Stock Centre. Homozygous lines were successfully identified (Supplementary Fig. S1); however, RT-PCR performed using *AtSLAH1*-specific primers (Supplementary Table S1) found that the expression of *AtSLAH1* was not abolished in these mutant lines (Supplementary Fig. S1C). Therefore, four independent amiRNA:*AtSLAH1* mutant lines were generated, which were named amiRNA:*AtSLAH1*_1 (two inserts), amiRNA:*AtSLAH1*_2 (two inserts), amiRNA:*AtSLAH1*_3 (three inserts) and amiRNA:*AtSLAH1*_4 (two inserts). Under low salt conditions (2 mM NaCl), qRT-PCR showed that the transcript abundance of *AtSLAH1* in the root of all independent amiRNA lines was less than half of that found in the null segregants ($P \leq 0.005$) (Fig. 2A). In all amiRNA:*AtSLAH1* lines, the shoot Cl⁻ concentration was significantly lower than that of the null segregants under low salt conditions, being reduced by 30–47% ($P \leq 0.005$) (Fig. 2B). The expression level of *AtSLAH1* was plotted against shoot Cl⁻ concentration for each plant and a highly significant positive relationship was observed with an R^2 of 0.89. The shoot NO₃⁻ concentration under low Cl⁻ supply was also determined and no difference was found between the mutants and the null segregants (Supplementary Fig. S3A), but the reduction in shoot Cl⁻ led to a significantly greater shoot NO₃⁻/Cl⁻ ratio in all mutants when compared with the null segregants (Fig. 2D). No differences were found in shoot biomass in any of the amiRNA:*AtSLAH1* lines under low Cl⁻ conditions (Supplementary Fig. S3B). The shoot Na⁺ and K⁺ concentrations were determined in these plants and no differences were found between all mutants and null segregants (Supplementary Fig. S3C, D). The experiment was repeated using the same set of seeds, under the same treatments, and found to have similar results where shoot Cl⁻ accumulation was decreased in amiRNA:*SLAH1* lines (Supplementary Fig. S3E). Under high Cl⁻ supply, amiRNA lines had significantly reduced *AtSLAH1* transcript abundance compared with the null segregants in the same conditions (Supplementary Fig. S4A); however, the *AtSLAH1* expression in the null segregants was reduced by a quarter compared with low Cl⁻ conditions (Fig. 1A and Supplementary Fig. S4A). At the same time there was no difference in shoot Cl⁻ concentration

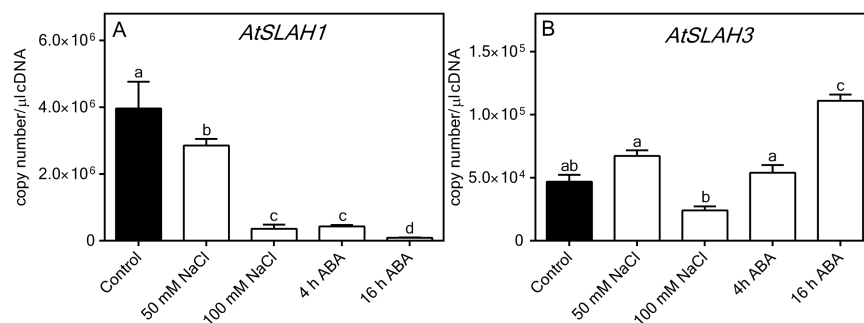


Fig. 1. Expression level of *AtSLAH1* (A) and *AtSLAH3* (B) treated with control (2 mM NaCl), 50 mM and 100 mM NaCl for 7 days, or 20 µM *cis-trans*-ABA for 4 or 16 h. Arabidopsis (Col-0) were grown in hydroponics for 5 weeks and exposed to NaCl treatment for 7 days. The ABA was applied 4 or 16 h before harvest. Transcripts were detected in the whole root cDNA. Results are presented as means ± SEM, $n=5$. The expression levels were normalized to four control genes (*AtGAPDH*, *AtActin2*, *AtTubulin* and *AtCyclophilin*). Statistical significance was determined by one-way analysis of variance (ANOVA) and Tukey's test ($P \leq 0.05$); a, b and c represent data groups that are statistically different from each other.

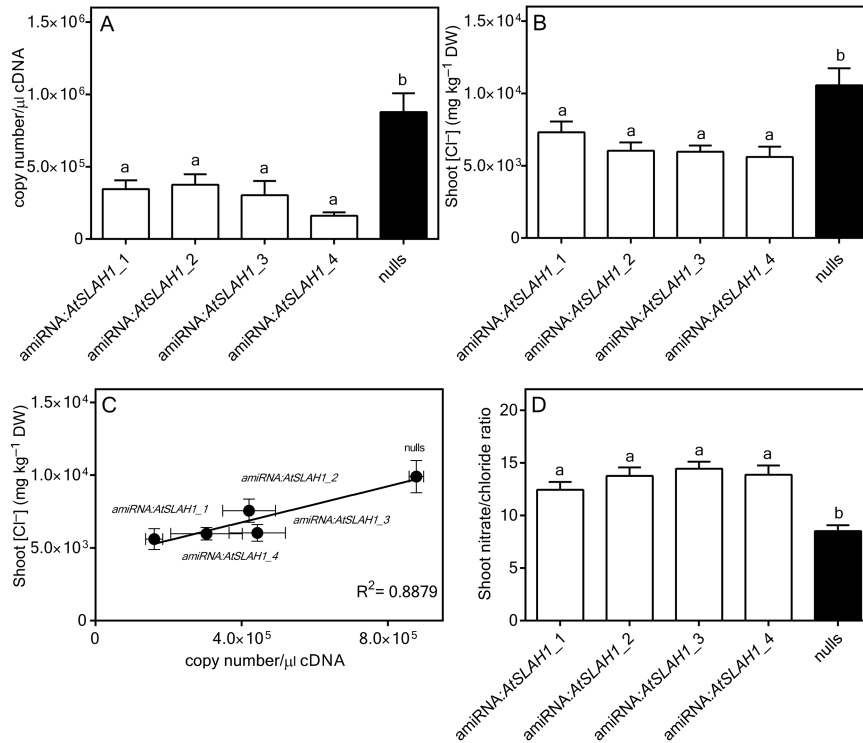


Fig. 2. Under low Cl^- conditions, amiRNA:*AtSLAH1* mutants had significantly reduced expression levels of *AtSLAH1* and reduced shoot Cl^- compared with null segregants. Plants were grown hydroponically for 6 weeks in BNS containing 2 mM NaCl (low Cl^- conditions). (A) *AtSLAH1* expression in roots of all amiRNA-*AtSLAH1* mutants (amiRNA:*AtSLAH1*_1, 2, 3 and 4) and null segregants (nulls). (B) Shoot Cl^- accumulation of amiRNA-*AtSLAH1* mutants and nulls under low Cl^- conditions. (C) Correlation between transcript level of *AtSLAH1* and shoot Cl^- concentration. (D) The shoot $\text{NO}_3^-/\text{Cl}^-$ ratio in all amiRNA:*AtSLAH1* mutant and null segregant lines grown under low Cl^- conditions. Results are mean \pm SEM ($n > 8$), except (C), which is \pm SEM. Statistical differences determined by one-way ANOVA and Tukey's test ($P \leq 0.005$); a and b represent statistically significant differences between data groups.

between the knockdown plants and controls under high Cl^- supply (Supplementary Fig. S4B). This was presumably due to the native downregulation of *AtSLAH1* expression by high salt (Figs 1A and 2A and Supplementary Fig. S4A).

Plants constitutively overexpressing *AtSLAH1* accumulate high Cl^- in the shoot under high Cl^- supply

Plants with constitutive overexpression of *AtSLAH1* and their null segregants were selected by determining the presence or absence of the *AtSLAH1* transgene by PCR of genomic DNA. Relative expression of total *AtSLAH1* (consisting of both the native and the transgenic *AtSLAH1*) was then determined in root tissue by semi-quantitative RT-PCR. *AtSLAH1* was found to be highly expressed in both *35S:AtSLAH1* lines generated, whereas the null segregants had less abundant expression (Fig. 3A). When 75 mM NaCl was applied to *35S:AtSLAH1*_1, *35S:AtSLAH1*_2 and null segregant lines for 7 days, significantly higher shoot Cl^- concentration accumulated in the overexpression lines when compared with the null segregants ($P \leq 0.05$), with no difference found between the two independent overexpression lines in shoot Cl^- concentration (Fig. 3B). The shoot NO_3^- in both overexpression lines displayed no differences compared with null segregants (Supplementary Fig. S5A). Therefore, the increase in shoot Cl^- accumulation resulted in a decrease in shoot $\text{NO}_3^-/\text{Cl}^-$ ratio in both overexpression lines under high Cl^- conditions ($P \leq 0.05$) (Fig. 3C). Both *35S:AtSLAH1* overexpression lines

had significantly less whole shoot biomass when compared with the null segregants ($P \leq 0.005$) (Fig. 3D).

Under low Cl^- supply, the shoot Cl^- and NO_3^- concentration of both *35S:AtSLAH1* overexpression lines was not significantly different from each other or the null segregants (Supplementary Fig. S5B, C), and the shoot biomass between all the genotypes was not significantly different (Supplementary Fig. S5D).

Stelar-specific overexpression of *AtSLAH1* is correlated with increased shoot Cl^- accumulation under high Cl^- supply

To further study the function of *AtSLAH1* and avoid potential problems caused by non-targeted over expression in all cell types, root stelar cell-type specific over expression lines were generated following the method outlined by Møller *et al.* 2009. Two independent lines, named *GAL4:AtSLAH1*_1 and *GAL4:AtSLAH1*_2 were grown in hydroponics for 6 weeks before being supplied with 2 or 75 mM NaCl for a further 7 days. Under high Cl^- conditions, both cell-specific overexpression lines had greater accumulation of Cl^- within the shoot; *AtSLAH1* expression and shoot Cl^- accumulation were again positively correlated ($R^2 = 0.5$, $P \leq 0.01$) (Fig. 4A). As with the constitutively overexpressing *AtSLAH1* plants, high salt treatment led to greater shoot Cl^- accumulation and no alteration in shoot concentration of Na^+ , K^+ or NO_3^- in the cell-specific overexpression lines compared to the null

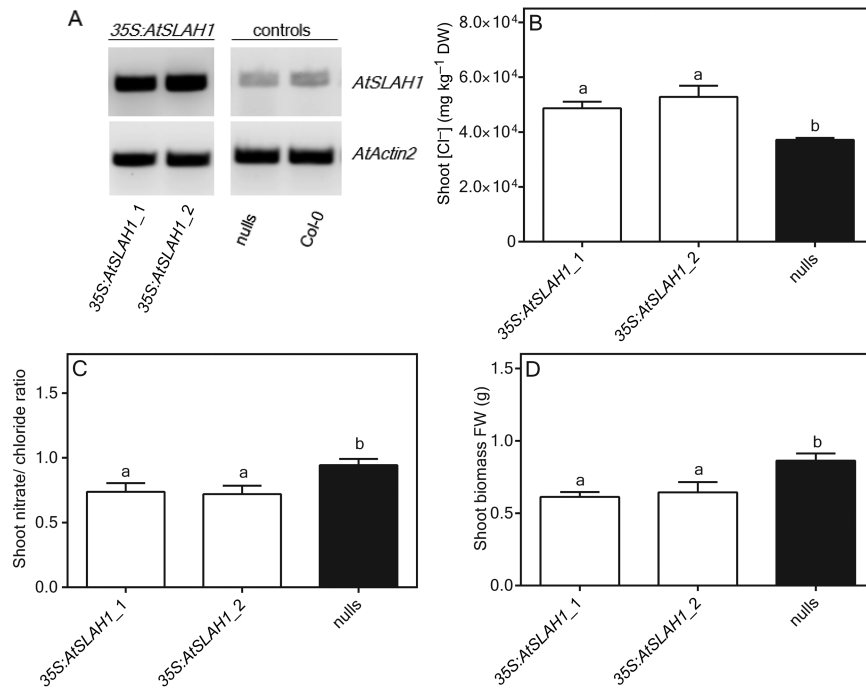


Fig. 3. Under high Cl^- conditions, *35S:AtSLAH1* overexpression lines accumulated higher shoot Cl^- and showed reduced $\text{NO}_3^-/\text{Cl}^-$ ratio compared with null segregants (nulls). Plants were grown hydroponically in BNS until 6 weeks old and then exposed to BNS containing 75 mM NaCl (high Cl^- conditions) for 7 days. (A) Semi-quantitative RT-PCR of *35S:AtSLAH1* overexpression lines and nulls. (B) Shoot Cl^- concentration under high Cl^- conditions. (C) Shoot $\text{NO}_3^-/\text{Cl}^-$ ratio. (D) Whole shoot biomass (fresh weight) as measured after high Cl^- treatment. Results are mean+SEM ($n>6$). Statistical differences determined by one-way ANOVA and Tukey's test ($P\leq 0.05$); a and b represent statistically significant differences between data groups.

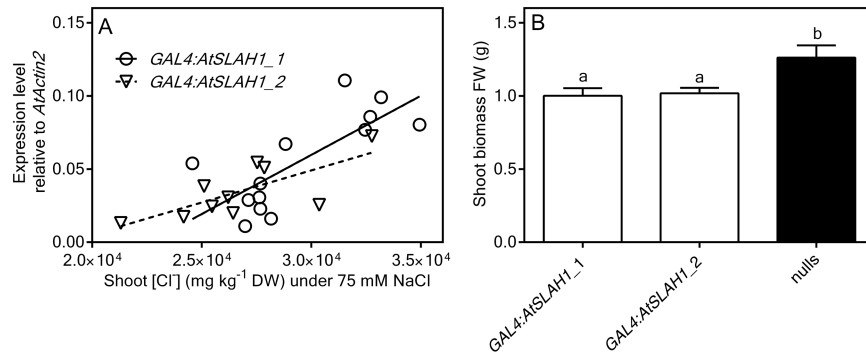


Fig. 4. Stelar cell type-specific overexpression of *AtSLAH1* in E2586 significantly increased shoot Cl^- accumulation and reduced shoot biomass under high Cl^- conditions. (A) Correlation between shoot Cl^- accumulation and relative expression of *AtSLAH1* in *GAL4:AtSLAH1* overexpression lines under high Cl^- (75 mM NaCl) supply. Open circles and solid line: *GAL4:AtSLAH1_1*; open triangle and dash line: *GAL4:AtSLAH1_2*. Plants were grown hydroponically in BNS for 6 weeks and then exposed to BNS containing 75 mM NaCl (high Cl^- conditions) for 7 days. Correlation between shoot Cl^- concentration and the abundance of *AtSLAH1* in *GAL4:AtSLAH1_1* ($R^2=0.5805$, $P\leq 0.005$, significant deviation from zero), *GAL4:AtSLAH1_2* ($R^2=0.5395$, $P\leq 0.005$, significant deviation from zero). (B) Whole shoot biomass (fresh weight) as measured after high Cl^- treatment. Results are mean+SEM ($n>6$). Statistical differences determined by one-way ANOVA and Tukey's test ($P\leq 0.05$); a and b represent statistically significant differences between data groups.

segregant lines (Supplementary Fig. S6A, B, C). Furthermore, the shoot biomass of the cell-specific overexpression lines was reduced under high salt treatment compared with the null segregants (Fig. 4B).

Under low Cl^- conditions, no significant differences in shoot Cl^- or NO_3^- accumulation were identified between stelar-specific *AtSLAH1* overexpression lines and the null segregants (Supplementary Fig. S7A, B), but significantly less shoot Cl^- was accumulated in these plants in low Cl^- than when in high Cl^- treatment (Fig. 4A). Under low Cl^- conditions, the shoot biomass of both stelar-specific *AtSLAH1*

overexpression lines was not significantly different from the null segregants (Supplementary Fig. S7C).

AtSLAH3 overexpression increases the shoot $\text{NO}_3^-/\text{Cl}^-$ ratio under high and low Cl^-

To compare the effects of *AtSLAH1* misexpression with that of a close homologue known to have a preference for NO_3^- transport, we examined the phenotype of plants constitutively overexpressing *AtSLAH3*. In contrast to the greater Cl^- accumulation we observed in shoots of *AtSLAH1*-overexpressing

plants, we observed a lower accumulation of shoot Cl⁻ under both high and low Cl⁻ supply in *AtSLAH3*-overexpressing plants (Supplementary Fig. S8A, B). The mean value for NO₃⁻ concentration of the shoot was higher in the overexpression lines (Supplementary Fig. S8C, D), but not significantly compared with the null segregants under any condition tested, but coupled to the Cl⁻ data led to a significantly greater NO₃⁻/Cl⁻ ratio in all conditions tested (Supplementary Fig. 8E, F).

AtSLAH1 is likely to require additional co-factors to be active in *X. laevis* oocytes

AtSLAH1 was expressed in *X. laevis* oocytes in an attempt to examine whether it could directly catalyse the transport Cl⁻ (Supplementary Materials and methods). No functional activity could be detected when *AtSLAH1* was expressed by itself (Supplementary Fig. S9). The *AtSLAH1* homologue, *AtSLAC1*, was also found to be electrically silent in oocytes when expressed by itself, but when expressed with *sucrose non-fermenting-1-related protein kinase 2.6* (*SnRK2.6*) *AtSLAC1* carried currents (Geiger *et al.*, 2009). To investigate whether a similar regulatory process was also required to trigger anion transport by *AtSLAH1* in heterologous systems, *AtSnRk2.2* and *AtSnRk2.3* (root localized homologues of *AtSnRk2.6* that have their expression regulated by ABA; Yoshida *et al.*, 2006; Fujii and Zhu, 2009; Nakashima *et al.*, 2009) were co-injected with *AtSLAH1* in *X. laevis* oocytes (Supplementary Fig. S9F–H) but this resulted in no consistent activation of current, suggesting additional cofactors that regulate SLAH1 function still need to be identified.

Discussion

AtSLAH1 meets the predicted characteristics for a gene controlling Cl⁻ loading into the root xylem

Previous studies showed that *AtSLAH1* belongs to the *AtSLAC1* family; *SLAC1* and *SLAH3* underpin components of the slow type (S-type) anion conductance involved in anion efflux across the PM of stomatal guard cells in response to CO₂ and O₃ (Negi *et al.*, 2008; Vahisalu *et al.*, 2008; Geiger *et al.*, 2011; Demir *et al.*, 2013). The guard cell PM S-type anion conductance was found to be permeable to malate, Cl⁻ and NO₃⁻ and its activation triggered by ABA (Schroeder and Hagiwara, 1989; Hedrich, 2012). *AtSLAH3* and another family member, *AtSLAH2*, have been predicted to load NO₃⁻ into the root stele (Maierhofer *et al.*, 2014; Zheng *et al.*, 2015). Whilst *AtSLAH1* is not usually expressed in guard cells it could complement the wild-type guard cell function of the *slac1* knockout when ectopically expressed, indicating it may encode or regulate a functional channel (Negi *et al.*, 2008; Vahisalu *et al.*, 2008); however, its true physiological functions are yet to be deciphered. Here, we confirmed that *AtSLAH1* was highly expressed in the Arabidopsis root and its expression was down-regulated strongly by ABA and NaCl treatment (Fig. 1). Previously *AtSLAH1* was shown to be expressed in the root stele and pericycle of Arabidopsis roots and present on the PM (Brady *et al.*, 2007; Gifford

et al., 2008; Negi *et al.*, 2008; Supplementary Fig. S2). As the stelar-localized PM conductances capable of loading anions into the root xylem (and consequently the shoot) have been observed to be down-regulated by ABA (Gilliham and Tester, 2005) this suggests that *AtSLAH1* could be involved in significant Cl⁻ loading of the root xylem. In contrast, we found that *AtSLAH3* transcript abundance was not reduced by salt or down-regulated by ABA (Fig. 1B). This coupled to the higher NO₃⁻/Cl⁻ ratio of *AtSLAH3*-overexpressing plants (Supplementary Fig. S8E and F) suggests it does not, by itself, contribute to a significant proportion of Cl⁻ accumulation in the shoot.

AtSLAH1 regulates Arabidopsis shoot Cl⁻ accumulation

As the '*Atslah1*' T-DNA insertion mutant from the European Arabidopsis Stock Centre retained expression of *SLAH1*, we generated amiRNA lines that had reduced expression of *AtSLAH1* (Fig. 2A). Under low Cl⁻ supply (2 mM NaCl), all *AtSLAH1* amiRNA lines had lower accumulation of Cl⁻ but not of NO₃⁻ in the shoot (Fig. 2A, B and Supplementary Fig. S3A). There was also a strong positive correlation between *AtSLAH1* expression levels and shoot Cl⁻ (Fig. 2C), which suggests that *AtSLAH1* might play an important role in regulating Cl⁻ transport from root to shoot by affecting net loading of xylem vessels in the root. Whilst the shoot NO₃⁻ concentration did not significantly alter when compared with the null segregants (Supplementary Fig. S3A), reduced *AtSLAH1* expression did lead to an increased shoot NO₃⁻/Cl⁻ ratio due to a lower amount of Cl⁻ in the shoot (Fig. 2D).

Shoot Cl⁻ concentration was also examined in all amiRNA:*AtSLAH1* mutants exposed to high salt stress. No shoot Cl⁻ concentration differences were found between mutants and the null segregants under these conditions (Supplementary Fig. S4B). *AtSLAH1* expression is naturally decreased under high concentrations of NaCl (Fig. 1A). Therefore it is reasonable to suggest that the unchanged shoot Cl⁻ concentration in these plants was probably due to the endogenous down-regulation of *AtSLAH1* caused by high salinity. Therefore, the results of *AtSLAH1* overexpression lines might be expected to be more instructive for determining *AtSLAH1* function under high salt conditions.

In *35S:AtSLAH1* overexpression lines we observed significantly increased shoot Cl⁻ accumulation compared with null segregants when grown under high Cl⁻ (75 mM NaCl) (Fig. 3B); this is again consistent with *AtSLAH1* being involved in xylem Cl⁻ loading. No difference in shoot NO₃⁻, K⁺ or Na⁺ accumulation was observed between *35S:AtSLAH1* overexpression lines and null segregants under high Cl⁻ supply (Supplementary Fig. S5A, E, F) indicating that the role of *AtSLAH1* is specific for Cl⁻. This translated into a reduced NO₃⁻/Cl⁻ ratio in these lines compared with nulls (Fig. 3C). In overexpression lines, there was a concomitant decrease in shoot biomass compared with null segregant lines (Fig. 3C), suggesting that the level of Cl⁻ accumulated, and the reduction in NO₃⁻/Cl⁻ ratio over this time period is sub-optimal for growth. In many studies, the shoot K⁺/Na⁺ ratio

is widely used to evaluate the plant's salt tolerance: a higher K^+/Na^+ ratio value normally indicates a better salinity tolerance (Tester and Davenport, 2003). Due to the antagonism between Cl^- and NO_3^- transport and the key roles of NO_3^- in plant metabolism, it is reasonable to suggest that mechanisms that maintain high NO_3^-/Cl^- ratios might also be beneficial for improving salt tolerance.

These effects on shoot Cl^- accumulation, shoot NO_3^-/Cl^- ratio and shoot biomass were replicated in *AtSLAH1* root stelar cell-specific overexpression lines in high Cl^- conditions (in the cell types in which *AtSLAH1* is ordinarily expressed (Brady *et al.*, 2007; Gifford *et al.*, 2008; Negi *et al.*, 2008) (Fig. 4). This indicates that constitutive overexpression of *AtSLAH1* did not result in significant pleiotropic responses, which may be to do with the need for an unknown interacting partner in its native cell type for *AtSLAH1* to be functional. What is important to note is that in *AtSLAH1* constitutively overexpressing plants and in the root stelar specific *AtSLAH1* overexpression lines in low Cl^- growth conditions, there was no growth phenotype compared with the null segregants (Figs 3 and 4). This linked to the fact that other ion contents (K^+ , Na^+ or NO_3^-) were not altered in any conditions (Supplementary Figs S5 and S6), demonstrates that the growth of *AtSLAH1*-overexpressing plants was not altered by overexpression of the *AtSLAH1* protein *per se*. Rather the inhibition of growth seen for *AtSLAH1*-overexpressing plants in high Cl^- was specifically due to the additional accumulation of Cl^- in the shoot (Figs 3 and 4).

Chloride accumulation in the shoot is a multigenic trait (White, 2001). We have shown that *AtSLAH1* is likely to make up a component of this, as it has a significant effect on shoot Cl^- accumulation (~20–40% in various conditions), which suggests that other Arabidopsis anion transport proteins might be involved in root to shoot Cl^- transport. Recently, NFP2.4, a transport protein localized to the PM of stelar cells, was found to be important for Cl^- but not for NO_3^- accumulation in shoots (Li *et al.*, 2016). *AtCCC* has also been shown to have an impact on shoot Cl^- accumulation (Colmenero-Flores *et al.*, 2007; Henderson *et al.*, 2015). However, *AtCCC* is predominantly localized to the Golgi and *trans*-Golgi network and so is unlikely to have a direct role in net loading of Cl^- into the xylem (Henderson *et al.*, 2015). Other candidates include transporters designated as NO_3^- permeable, but which may also transport some Cl^- , such as NRT1.5/NPF7.3, NRT1.8/NPF7.2 and SLAH3 (Lin *et al.*, 2008; Li *et al.*, 2010). A transcriptional comparison between the roots of good and poor Cl^- -excluding grapevine rootstocks suggested further candidate genes for this multigenic trait including aluminium-activated malate transporters (ALMT), chloride channels (CLC) and their putative activating kinases (Henderson *et al.*, 2014). However, the true involvement of these candidate proteins requires that their substrates are resolved by functional assays. Therefore, the observed phenotypes in any single gene mutant are likely to be complicated by other functional proteins involved in Cl^- accumulation in the shoot.

AtSLAH1 is likely to require unknown interacting proteins to function

No anion-mediated currents were identified when *AtSLAH1* cRNA was injected into *X. laevis* oocytes (Supplementary Fig. S9C, D). *AtSLAC1*, *AtSLAH2* and *AtSLAH3* are known to require protein kinases to be functional in oocytes (Geiger *et al.*, 2009; Vahisalu *et al.*, 2010; Brandt *et al.*, 2012; Demir *et al.*, 2013; Gutermuth *et al.*, 2013; Maierhofer *et al.*, 2014). For instance, when *SLAC1* was expressed in *X. laevis* oocytes no clear anion currents were generated (Vahisalu *et al.*, 2008); however, co-expression with the protein kinase SnRk2.6 in oocytes was found to activate *SLAC1* by phosphorylation of multiple serines in the *SLAC1* hydrophilic N-terminal sequence (Geiger *et al.*, 2009; Lee *et al.*, 2009; Vahisalu *et al.*, 2010). This evidence suggests that a similar regulatory component is important for activating the S-type anion channels and may be required for *SLAH1* activity. As SnRK2.6 has low expression in roots we concentrated on the root expressed members of the ABA-activated SNF1-related protein kinases 2, SnRK2.2 and SnRK2.3, which are both involved in ABA signalling pathways in roots (Yoshida *et al.*, 2006; Fujii and Zhu, 2009; Nakashima *et al.*, 2009). To identify whether a phosphorylation process initiated by a protein kinase was required to activate *SLAH1* in oocytes, SnRK2.2/2.3 was co-injected with *AtSLAH1* into oocytes (Supplementary Fig. S9G–J). However, no activity was observed. Therefore, it is likely that *AtSLAH1* requires additional factors for it to be active, or that it is itself a regulator of transport through its interaction with another transport protein.

Conclusions

Manipulating *AtSLAH1* expression level in Arabidopsis resulted in significant alterations in shoot Cl^- concentrations suggesting *AtSLAH1* is involved in Cl^- xylem loading in roots and the regulation of Cl^- accumulation in the shoot in response to salt stress. In contrast, overexpression of *AtSLAH3* resulted in relatively greater NO_3^- content of the shoot under low and high Cl^- treatments. In the present work, heterologous expression studies were unable to distinguish whether *AtSLAH1* acts directly as a transport protein or transport regulator. As *AtSLAH1* expression decreases under salinity and ABA, but *AtSLAH3* is still expressed, the relative capacity for roots to deliver NO_3^- to the shoot is increased under saline conditions but the capacity for Cl^- loading is reduced. This will serve to maximize important NO_3^- delivery to the shoot despite the increased competition from Cl^- during salinity stress. Therefore, it appears likely that *AtSLAH1* and *AtSLAH3* act in tandem to regulate NO_3^- and Cl^- loading to the shoot and are both targets for manipulation in crops to improve salinity tolerance.

Supplementary data

Supplementary data are available at *JXB* online.

Figure S1. *AtSLAH1* is still expressed in the *slah1* homozygous T-DNA insertion line FLAG_336C06.

Figure S2. The transcript level changes of *AtSLAH1* and *AtSLAH3* upon NaCl or ABA treatment.

Figure S3. Under low Cl⁻ conditions, the shoot NO₃⁻, Na⁺, K⁺ concentrations and biomass were detected in all amiRNA:*AtSLAH1* mutants and null segregants (nulls).

Figure S4. Transcript abundance of *AtSLAH1* amiRNA containing lines (T₂) and shoot Cl⁻ concentration under high Cl⁻ stress.

Figure S5. The shoot NO₃⁻, Cl⁻ concentrations and shoot biomass were detected under low and high Cl⁻ supply in both *35S:AtSLAH1_1* and *35S:AtSLAH1_2*, and null segregants (nulls).

Figure S6. Under high Cl⁻ conditions, the shoot Na⁺, K⁺ and NO₃⁻ concentrations were detected in all *GALA:AtSLAH1* overexpression lines and null segregants (nulls).

Figure S7. Under low Cl⁻ conditions, shoot Cl⁻, NO₃⁻ concentrations and whole shoot biomass were detected in all *GALA:AtSLAH1* overexpression lines and null segregant.

Figure S8. The shoot NO₃⁻ and Cl⁻ concentrations were detected under low and high Cl⁻ supply in both *35S:AtSLAH3_1* and *35S:AtSLAH3_2*, and null segregant (nulls) lines.

Figure S9. Electrophysiological characterization of *AtSLAH1* in *X. laevis* oocytes.

Table S1. Primers used for generating amiRNA:*AtSLAH1* constructs, for screening homozygous *Atslah1* T-DNA mutant lines and for cloning *AtSLAH1/AtSLAH3* from Arabidopsis.

Acknowledgements

The authors thank Dr Darren Plett for donating the destination vector (pTOOL5) in this study; Yuan Li and Hui Zhou for performing the qRT-PCRs (Australian Centre for Plant Function Genomics, Adelaide, Australia). The work was supported by: the Grains Research and Development Corporation (UA000145 to S.J.R., M.G.); the Australian Research Council (ARC) through Centre of Excellence (CE14010008) and Future Fellowship (FT130100709) funding to M.G.; and, the University of Adelaide Graduate Research Scholarship and the Australian Centre for Plant Functional Genomics student scholarship to J.Q.

References

- Abel GH. 1969. Inheritance of capacity for chloride inclusion and chloride exclusion by soybeans. *Crop Science* **9**, 697–698.
- Apse MP, Blumwald E. 2007. Na⁺ transport in plants. *FEBS Letters* **581**, 2247–2254.
- Blumwald E, Aharon GS, Apse MP. 2000. Sodium transport in plant cells. *Biochimica et Biophysica Acta* **1465**, 140–151.
- Brady SM, Orlando DA, Lee J-Y, Wang JY, Koch J, Dinneny JR, Mace D, Ohler U, Benfey PN. 2007. A high-resolution root spatiotemporal map reveals dominant expression patterns. *Science* **318**, 801–806.
- Brandt B, Brodsky DE, Xue S, Negi J, Iba K, Kangasjarvi J, Ghassemian M, Stephan AB, Hu H, Schroeder JI. 2012. Reconstitution of abscisic acid activation of SLAC1 anion channel by CPK6 and OST1 kinases and branched ABI1 PP2C phosphatase action. *Proceedings of the National Academy of Sciences of the United States of America* **109**, 10593–10598.
- Broadley M, Brown P, Cakmak I, Rengel Z, Zhao F. 2012. Function of nutrients: micronutrients. In Marschner P, ed. *Mineral nutrition of higher plants*. London: Academic Press, 191–248.
- Burton RA, Jobling SA, Harvey AJ, Shirley NJ, Mather DE, Bacic A, Fincher GB. 2008. The genetics and transcriptional profiles of the cellulose synthase-like HvCslF gene family in barley. *Plant Physiology* **146**, 1821–1833.
- Cataldo DA, Haroon M, Schrader LE, Youngs VL. 1975. Rapid colorimetric determination of nitrate in plant-tissue by nitration of salicylic-acid. *Communications in Soil Science and Plant Analysis* **6**, 71–80.
- Chen Y, Hu L, Punta M, Bruni R, Hillerich B, Kloss B, Rost B, Love J, Siegelbaum SA, Hendrickson WA. 2010. Homologue structure of the SLAC1 anion channel for closing stomata in leaves. *Nature* **467**, 1074–1080.
- Chinnusamy V, Zhu J, Zhu J-K. 2006. Salt stress signaling and mechanisms of plant salt tolerance. *Genetic Engineering* **27**, 141–177.
- Clough SJ, Bent AF. 1998. Floral dip: a simplified method for *Agrobacterium*-mediated transformation of *Arabidopsis thaliana*. *The Plant Journal* **16**, 735–743.
- Colmenero-Flores JM, Martinez G, Gamba G, Vazquez N, Iglesias DJ, Brumos J, Talon M. 2007. Identification and functional characterization of cation-chloride cotransporters in plants. *The Plant Journal* **50**, 278–292.
- Conn SJ, Hocking B, Dayod M, et al. 2013. Protocol: optimising hydroponic growth systems for nutritional and physiological analysis of *Arabidopsis thaliana* and other plants. *Plant Methods* **9**, 4.
- Cram WJ, Pitman MG. 1972. Action of abscisic acid on ion uptake and water flow in plant roots. *Australian Journal of Biological Sciences* **25**, 1125–1132.
- Curtis MD, Grossniklaus U. 2003. A gateway cloning vector set for high-throughput functional analysis of genes in planta. *Plant Physiology* **133**, 462–469.
- Davenport R, James RA, Zakrisson-Plogander A, Tester M, Munns R. 2005. Control of sodium transport in durum wheat. *Plant Physiology* **137**, 807–818.
- Demir F, Horntrich C, Blachutzik JO, Scherzer S, Reinders Y, Kierszniowska S, Schulze WX, Harms GS, Hedrich R, Geiger D, Kreuzer I. 2013. Arabidopsis nanodomain-delimited ABA signaling pathway regulates the anion channel SLAH3. *Proceedings of the National Academy of Sciences of the United States of America* **110**, 8296–8301.
- Flowers TJ, Munns R, Colmer TD. 2015. Sodium chloride toxicity and the cellular basis of salt tolerance in halophytes. *Annals of Botany* **115**, 419–431.
- Fort KP, Heinitz CC, Walker MA. 2015. Chloride exclusion patterns in six grapevine populations. *Australian Journal of Grape and Wine Research* **21**, 147–155.
- Franco-Navarro JD, Brumós J, Rosales MA, Cubero-Font P, Talón M, Colmenero-Flores JM. 2015. Chloride regulates leaf cell size and water relations in tobacco plants. *Journal of Experimental Botany* **67**, 873–891.
- Fujii H, Zhu JK. 2009. Arabidopsis mutant deficient in 3 abscisic acid-activated protein kinases reveals critical roles in growth, reproduction, and stress. *Proceedings of the National Academy of Sciences of the United States of America* **106**, 8380–8385.
- Garthwaite AJ, von Bothmer R, Colmer TD. 2005. Salt tolerance in wild *Hordeum* species is associated with restricted entry of Na⁺ and Cl⁻ into the shoots. *Journal of Experimental Botany* **56**, 2365–2378.
- Gaymard F, Pilot G, Lacombe B, Bouchez D, Bruneau D, Bouchez J, Michaux-Ferriere N, Thibaud JB, Sentenac H. 1998. Identification and disruption of a plant shaker-like outward channel involved in K⁺ release into the xylem sap. *Cell* **94**, 647–655.
- Geiger D, Maierhofer T, Al-Rasheid KAS, et al. 2011. Stomatal closure by fast abscisic acid signaling is mediated by the guard cell anion channel SLAH3 and the receptor RCAR1. *Science Signaling* **4**, ra32.
- Geiger D, Scherzer S, Mumm P, et al. 2009. Activity of guard cell anion channel SLAC1 is controlled by drought-stress signaling kinase-phosphatase pair. *Proceedings of the National Academy of Sciences of the United States of America* **106**, 21425–21430.
- Genc Y, Oldach K, Taylor J, Lyons GH. 2015. Uncoupling of sodium and chloride to assist breeding for salinity tolerance in crops. *New Phytologist* **210**, 145–156.
- Gifford ML, Dean A, Gutierrez RA, Coruzzi GM, Birnbaum KD. 2008. Cell-specific nitrogen responses mediate developmental plasticity. *Proceedings of the National Academy of Sciences of the United States of America* **105**, 803–808.

- Gilliham M, Tester M.** 2005. The regulation of anion loading to the maize root xylem. *Plant Physiology* **137**, 819–828.
- Gong H, Blackmore D, Clingeffer P, Sykes S, Jha D, Tester M, Walker R.** 2011. Contrast in chloride exclusion between two grapevine genotypes and its variation in their hybrid progeny. *Journal of Experimental Botany* **62**, 989–999.
- Gutermuth T, Lassig R, Portes MT, Maierhofer T, Romeis T, Borst JW, Hedrich R, Feijo JA, Konrad KR.** 2013. Pollen tube growth regulation by free anions depends on the interaction between the anion channel SLAH3 and calcium-dependent protein kinases CPK2 and CPK20. *The Plant Cell* **25**, 4525–4543.
- Harrison SJ, Mott EK, Parsley K, Aspinall S, Gray JC, Cottage A.** 2006. A rapid and robust method of identifying transformed *Arabidopsis thaliana* seedlings following floral dip transformation. *Plant Methods* **2**, 19–25.
- Hedrich R.** 2012. Ion channels in plants. *Physiological Reviews* **92**, 1777–1811.
- Henderson SW, Baumann U, Blackmore DH, Walker AR, Walker RR, Gilliham M.** 2014. Shoot chloride exclusion and salt tolerance in grapevine is associated with differential ion transporter expression in roots. *BMC Plant Biology* **14**, 273–291.
- Henderson SW, Wege S, Qiu J, Blackmore DH, Walker AR, Tyerman SD, Walker RR, Gilliham M.** 2015. Grapevine and *Arabidopsis* cation-chloride cotransporters localize to the Golgi and trans-Golgi network and indirectly influence long-distance ion transport and plant salt tolerance. *Plant Physiology* **169**, 2215–2229.
- Horie T, Schroeder JI.** 2004. Sodium transporters in plants. Diverse genes and physiological functions. *Plant Physiology* **136**, 2457–2462.
- Horie T, Sugawara M, Okunou K, Nakayama H, Schroeder JI, Shinmyo A, Yoshida K.** 2008. Functions of HKT transporters in sodium transport in roots and in protecting leaves from salinity stress. *Plant Biotechnology* **25**, 233–239.
- Jha D, Shirley N, Tester M, Roy SJ.** 2010. Variation in salinity tolerance and shoot sodium accumulation in *Arabidopsis* ecotypes linked to differences in the natural expression levels of transporters involved in sodium transport. *Plant Cell and Environment* **33**, 793–804.
- Kiegle E, Gilliham M, Haseloff J, Tester M.** 2000. Hyperpolarisation-activated calcium currents found only in cells from the elongation zone of *Arabidopsis thaliana* roots. *The Plant Journal* **21**, 225–229.
- Kilian J, Whitehead D, Horak J, Wanke D, Weini S, Batistic O, D'Angelo C, Bornberg-Bauer E, Kudla J, Harter K.** 2007. The AtGenExpress global stress expression data set: protocols, evaluation and model data analysis of UV-B light, drought and cold stress responses. *The Plant Journal* **50**, 347–363.
- Köhler B, Raschke K.** 2000. The delivery of salts to the xylem. Three types of anion conductance in the plasmalemma of the xylem parenchyma of roots of barley. *Plant Physiology* **122**, 243–254.
- Köhler B, Wegner LH, Osipov V, Raschke K.** 2002. Loading of nitrate into the xylem: apoplastic nitrate controls the voltage dependence of X-QUAC, the main anion conductance in xylem-parenchyma cells of barley roots. *The Plant Journal* **30**, 133–142.
- Lee LY, Lan W, Buchanan BB, Luan S.** 2009. A protein kinase-phosphatase pair interacts with an ion channel to regulate ABA signaling in plant guard cells. *Proceedings of the National Academy of Sciences of the United States of America* **106**, 21419–21424.
- Li B, Byrt C, Qiu J, Baumann U, Hrmova M, Evrard A, Johnson AAT, Birnbaum KD, Mayo GM, Jha D, Henderson SW, Tester M, Gilliham M, Roy SJ.** 2016. Identification of a stelar-localized transport protein that facilitates root-to-shoot transfer of chloride in *Arabidopsis*. *Plant Physiology* **170**, 1014–1029.
- Li JY, Fu YL, Pike SM, et al.** 2010. The *Arabidopsis* nitrate transporter NRT1.8 functions in nitrate removal from the xylem sap and mediates cadmium tolerance. *The Plant Cell* **22**, 1633–1646.
- Lin SH, Kuo HF, Canivenc G, et al.** 2008. Mutation of the *Arabidopsis* NRT1.5 nitrate transporter causes defective root-to-shoot nitrate transport. *The Plant Cell* **20**, 2514–2528.
- Linder B, Raschke K.** 1992. A slow anion channel in guard-cells, activating at large hyperpolarization, may be principal for stomatal closing. *FEBS Letters* **313**, 27–30.
- Maathuis FJ, Ahmad I, Patishtan J.** 2014. Regulation of Na⁺ fluxes in plants. *Frontiers in Plant Science* **5**, 467.
- Maierhofer T, Diekmann M, Offenborn JN, et al.** 2014. Site- and kinase-specific phosphorylation-mediated activation of SLAC1, a guard cell anion channel stimulated by abscisic acid. *Science Signaling* **7**, ra86.
- Marschner H.** 1995. Mineral nutrition of higher plants, 2nd edn. Houston: Gulf Professional Publishing.
- Møller IS, Gilliham M, Jha D, Mayo GM, Roy SJ, Coates JC, Haseloff J, Tester M.** 2009. Shoot Na⁺ exclusion and increased salinity tolerance engineered by cell type-specific alteration of Na⁺ transport in *Arabidopsis*. *The Plant Cell* **21**, 2163–2178.
- Moya JL, Gomez-Cadenas A, Primo-Millo E, Talon M.** 2003. Chloride absorption in salt-sensitive Carrizo citrange and salt-tolerant Cleopatra mandarin citrus rootstocks is linked to water use. *Journal of Experimental Botany* **54**, 825–833.
- Müller M, Kunz HH, Schroeder JI, Kemp G, Young HS, Neuhaus HE.** 2014. Decreased capacity for sodium export out of *Arabidopsis* chloroplasts impairs salt tolerance, photosynthesis and plant performance. *The Plant Journal* **78**, 646–658.
- Munns R, Gilliham M.** 2015. Salinity tolerance of crops – what is the cost? *New Phytologist* **208**, 668–673.
- Nakashima K, Fujita Y, Kanamori N, et al.** 2009. Three *Arabidopsis* SnRK2 protein kinases, SRK2D/SnRK2.2, SRK2E/SnRK2.6/OST1 and SRK2I/SnRK2.3, involved in ABA signaling are essential for the control of seed development and dormancy. *Plant and Cell Physiology* **50**, 1345–1363.
- Negi J, Matsuda O, Nagasawa T, Oba Y, Takahashi H, Kawai-Yamada M, Uchimiya H, Hashimoto M, Iba K.** 2008. CO₂ regulator SLAC1 and its homologues are essential for anion homeostasis in plant cells. *Nature* **452**, 483–486.
- Pitman MG.** 1982. Transport across plant roots. *Quarterly Reviews of Biophysics* **15**, 481–554.
- Plett DC.** 2008. Spatial and temporal alterations of gene expression in rice. Ph.D. Thesis, University of Adelaide.
- Preuss CP, Huang CY, Tyerman SD.** 2011. Proton-coupled high-affinity phosphate transport revealed from heterologous characterization in *Xenopus* of barley-root plasma membrane transporter, HvPHT1;1. *Plant Cell and Environment* **34**, 681–689.
- Rengasamy P.** 2010. Soil processes affecting crop production in salt-affected soils. *Functional Plant Biology* **37**, 613–620.
- Rognes SE.** 1980. Anion regulation of lupin asparagine synthetase-chloride activation the glutamine-utilizing reactions. *Phytochemistry* **19**, 2287–2293.
- Roy SJ, Gilliham M, Berger B, et al.** 2008. Investigating glutamate receptor-like gene co-expression in *Arabidopsis thaliana*. *Plant Cell and Environment* **31**, 861–871.
- Roy SJ, Negro S, Tester M.** 2014. Salt resistant crop plants. *Current Opinion in Biotechnology* **26**, 115–124.
- Schroeder JI, Hagiwara S.** 1989. Cytosolic calcium regulates ion channels in the plasma-membrane of *Vicia faba* guard-cells. *Nature* **338**, 427–430.
- Schwab R, Ossowski S, Riester M, Warthmann N, Weigel D.** 2006. Highly specific gene silencing by artificial microRNAs in *Arabidopsis*. *The Plant Cell* **18**, 1121–1133.
- Sibole JV, Cabot C, Poschenrieder C, Barcelo J.** 2003. Efficient leaf ion partitioning, an overriding condition for abscisic acid-controlled stomatal and leaf growth responses to NaCl salinization in two legumes. *Journal of Experimental Botany* **54**, 2111–2119.
- Storey R, Walker RR.** 1999. Citrus and salinity. *Scientia Horticulturae* **78**, 39–81.
- Tavakkoli E, Fatehi F, Coventry S, Rengasamy P, McDonald GK.** 2011. Additive effects of Na⁺ and Cl⁻ ions on barley growth under salinity stress. *Journal of Experimental Botany* **62**, 2189–2203.
- Teakle NL, Flowers TJ, Real D, Colmer TD.** 2007. Lotus tenuis tolerates the interactive effects of salinity and waterlogging by 'excluding' Na⁺ and Cl⁻ from the xylem. *Journal of Experimental Botany* **58**, 2169–2180.
- Teakle NL, Tyerman SD.** 2010. Mechanisms of Cl⁻ transport contributing to salt tolerance. *Plant Cell and Environment* **33**, 566–589.
- Tester M, Davenport R.** 2003. Na⁺ tolerance and Na⁺ transport in higher plants. *Annals of Botany* **91**, 503–527.
- Tregeagle JM, Tisdall JM, Blackmore DH, Walker RR.** 2006. A diminished capacity for chloride exclusion by grapevine rootstocks

following long-term saline irrigation in an inland versus a coastal region of Australia. *Australian Journal of Grape and Wine Research* **12**, 178–191.

Vahisalu T, Kollist H, Wang YF, et al. 2008. SLAC1 is required for plant guard cell S-type anion channel function in stomatal signalling. *Nature* **452**, 487–491.

Vahisalu T, Puzorjova I, Brosche M, et al. 2010. Ozone-triggered rapid stomatal response involves the production of reactive oxygen species, and is controlled by SLAC1 and OST1. *The Plant Journal* **62**, 442–453.

Walker RR, Blackmore DH, Clingeleffer PR, Correll RL. 2002. Rootstock effects on salt tolerance of irrigated field-grown grapevines (*Vitis vinifera* L. cv. Sultana). 1. Yield and vigour inter-relationships. *Australian Journal of Grape and Wine Research* **8**, 3–14.

White PJ. 2001. The pathways of calcium movement to the xylem. *Journal of Experimental Botany* **52**, 891–899.

White PJ, Broadley MR. 2001. Chloride in soils and its uptake and movement within the plant: A review. *Annals of Botany* **88**, 967–988.

Xu GH, Magen H, Tarchitzky J, Kafkafi U. 2000. Advances in chloride nutrition of plants. *Advances in Agronomy* **68**, 97–150.

Yoshida R, Umezawa T, Mizoguchi T, Takahashi S, Takahashi F, Shinozaki K. 2006. The regulatory domain of SRK2E/OST1/SnRK2.6 interacts with ABI1 and integrates abscisic acid (ABA) and osmotic stress signals controlling stomatal closure in *Arabidopsis*. *Journal of Biological Chemistry* **281**, 5310–5318.

Zheng X, He K, Kleist T, Chen F, Luan S. 2015. Anion channel SLAH3 functions in nitrate-dependent alleviation of ammonium toxicity in *Arabidopsis*. *Plant Cell and Environment* **38**, 474–486.

Zhu JK. 2003. Regulation of ion homeostasis under salt stress. *Current Opinion in Plant Biology* **6**, 441–445.